TRACING COSMIC ACCRETION THROUGH THE XMM-NEWTON MEDIUM SURVEY (XMS)

X. Barcons, F.J. Carrera & M.T. Ceballos

Instituto de Física de Cantabria (CSIC-UC), 39005 Santander, Spain

ABSTRACT

We discuss the XMM-Newton Medium Survey (XMS), a large serendipitous X-ray source sample at intermediate X-ray fluxes which is where most of the energy from accretion onto super-massive black holes is released. The XMS is now spectroscopically identified to 85%, and this enables us to study a number of statistical properties of the X-ray source population at these fluxes.

Key words: Active Galactic Nuclei, X-ray Surveys.

1. INTRODUCTION

Serendipitous X-ray source surveys conducted with the help of XMM-Newton observations are yielding a detailed picture of the contents of the X-ray sky, in particular at high galactic latitudes (Watson et al 2001). Although the limited spatial resolution of XMM-Newton does not allow these surveys to go as deep as the ones conducted with Chandra (see Brandt & Hasinger 2005 for a review), the larger collecting area of XMM-Newton along with the larger field of view of the EPIC cameras make XMM-Newton optimum to conduct surveys at intermediate and bright fluxes. At the same time, the large effective area of XMM-Newton ensures that enough counts are accumulated in many of the sources detected as to conduct - at least a simple - spectroscopic analysis.

The XMM-Newton Medium Survey (XMS) was among the first serendipitous X-ray surveys to be started with XMM-Newton. It began as part of the AXIS[1] programme, where a large number of X-ray sources at all galactic latitudes and of various brightness were imaged in the optical and spectroscopically identified. The XMS is a flux limited survey in the 0.5-4.5 keV band (the band was chosen to optimize the sensitivity of XMM-Newton), with a limit of $2 \times 10^{-14}\,\mathrm{erg\,cm^{-2}\,s^{-1}}$. This implies a source density around 100 sources deg^{-2} and optical counterparts that in their majority are accessible for optical spectroscopy from 4m class telescopes.

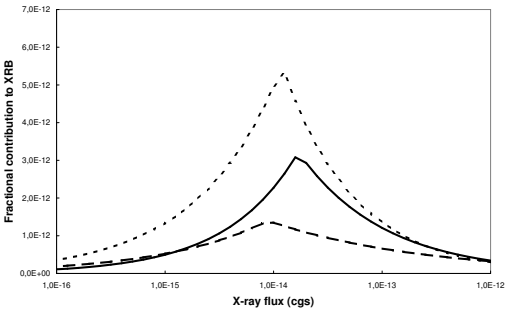

Figure 1. Differential contribution (in arbitrary units) to the XRB per flux decade in the 0.5-2 keV (dashed), 0.5-4.5 keV (continuous) and 2-10 keV (dotted).

There are a number of reasons on why such surveys are important. The first one is that they are needed to bridge the gap between the deep surveys (Hasinger et al 2001, Brandt & Hasinger 2005) and the more local bright surveys (Della Ceca et al 2004, Caccianiga et al 2004). A second reason is that the XMM-Newton source catalogue (of which the first version 1XMM was released in April 2003, and the second one is expected in 2006 containing between 100,000 and 150,000 X-ray sources) is in itself a huge medium sensitivity sample, given the average exposure time of the XMM-Newton observations. By building the XMS we can therefore know how to characterize, and possibly classify, most of the sources in the XMM-Newton catalogue. But possibly the most important reason to pay attention to intermediate flux surveys is that most of the Cosmic X-ray Background (XRB, see Fabian & Barcons 1992, for a still valid review) arises at these fluxes. Fig. 1 shows the fractional contribution to the XRB per flux decade at different fluxes and for various X-ray energy bands, where it is clear that most of the action occurs around intermediate fluxes. More specifically, with the most recent source counts, the XMS

[1] An XMM-Newton International Survey, http://www.ifca.unican.es/~xray/AXIS

resolves about 50% of the XRB in its own 0.5-4.5 keV energy band.

In this paper we summarize the XMS and its optical identification status (section 2), the content of the XMS (section 3) and some prospects on statistical identification based upon X-ray and optical colour information (section 4).

2. THE XMS AND ITS OPTICAL IDENTIFICATION

The XMS has been built from a parent serendipitous source list built from 25 XMM-Newton pointings. The fields were selected according to a number of criteria, including being at high galactic latitude ($\mid b \mid > 20^{\circ}$), the EPIC-pn observations being in full frame mode, having a resulting Good Time Interval in this instrument larger than 10 ks, not containing very bright (either in X-rays or in the optical) sources, the target itself not being too much extended and being available early on in the mission. This last point was important, as the first observations were carried out in April 2000.

The data have been reprocessed using the latest available version of the SAS (6.1.1) and best available calibration. This SAS version was used to produce exposure and background maps as well as to search for X-ray sources in the EPIC-pn field of view. Regions around the target, the CCD gaps (where gaps were broadened a bit) and near the pn "Out of Time events" trails were excluded from any further analysis and the corresponding solid angle not computed in the survey. To conduct any X-ray spectral analysis, events were extracted from all 3 EPIC detectors for each source, calibration matrices produced and background spectra extracted. We also constructed empirical sensitivity maps from detected source parameters, from which we computed solid angles. The EPIC-pn source lists were screened in detail to prevent any spurious source entering the final source list.

After this filtering process, the XMS contains 284 X-ray sources brighter than $2 \times 10^{-14}\,\mathrm{erg\,cm^{-2}\,s^{-1}}$ in the 0.5-4.5 keV band, covering a solid angle of 3.3 deg^2.

To conduct the optical identification of this sample, we first performed optical imaging of the XMM-Newton fields. In all fields but 1, we used the 2.5m INT within the AXIS programme. Sloan filters g', r' and i' were used in all cases, and in a fraction of them we also obtained images with the u(RGO) and Z (Gunn) filters. The approximate depth of the images is $\sim 23-24$ (depending on seeing, airmass and sky brightness) in r'.

Candidate counterparts for each XMS source were searched for in the r' images (primarily). These X-ray source lists were first registered to the USNO A2 reference frame by applying a possible shift to their coordinates after a number of matches in every field were found. Around the corrected X-ray source positions, candidate optical counterparts were considered if their position was within a 5σ error circle from the X-ray source (σ is the statistical error in the centroid of the X-ray position, the optical positions being much more accurate) or within 5". With this selection criteria the vast majority of the XMS sources had a unique and unambiguous candidate counterpart. Barcons et al (2002) presented the analysis of a 10 times smaller XMS based on 2 XMM-Newton fields only.

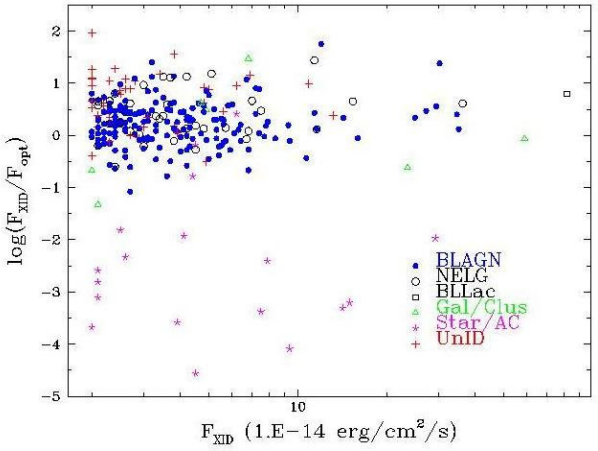

Figure 2. X-ray to optical flux ratio versus 0.5-4.5 keV X-ray flux for the XMS sources. Filled dots are BLAGN, hollow circles are NELGs, triangles are ALGs, asterisks are stars and crosses are unidentified sources.

Table 1. Breakdown of XMS sources.

Sources	Number	%
X-ray	284	100
Identified	242	85
Unid $r' < 20$	6	2.5
Unid $20 < r' < 21$	6	2.5
Unid $21 < r' < 22$	4	1.5
Unid $r' > 22$	26	9
Unid $Noimage$	1	0

Optical spectroscopy was then conducted to properly identify the sources. The AXIS programme provided about 50% of the XMS identifications with the use of fibre and long-slit spectrographs at the 4.2m WHT, the 3.5m TNG and the 2.6m NOT. A further 20% of identifications were obtained in 3 successive runs at the 3.5m telescope in the Spanish German Astronomical Centre in Calar Alto. A further $\sim 15\%$ of the identifications were obtained in a run at the VLT, especially those with a faint optical counterpart. A handful of additional sources had been identified in a variety of telescopes (AAT, SUBARU, etc.). Table 1 shows the breakdown of unidentified sources, classified in terms of their optical magnitude.

The XMS is therefore identified to 85%. There is however an obvious residual bias which is reflected in Tab. 1, as 9% of the full sample remains unidentified and the optical counterparts are fainter than $r' = 22$. These sources cannot be identified with a 4m class telescope, and they are all in the North and unaccessible from the VLT. The impact of these sources is also seen in Fig. 2, as they show up as relatively large F_X/F_{opt} sources, particularly at the faint end of our survey. This very fact implies that some conclusions from the present work are to be considered preliminary until a larger fraction of these sources are spectroscopically identified.

3. THE CONTENT OF THE XMS

3.1. Source counts

We used the full X-ray source lists in the XMM-Newton XMS fields along with the Bright Source Survey (BSS, Della Ceca et al 2004) to build source counts in the 0.5-4.5 keV. Although both surveys operate in the same band, our source lists are derived from EPIC-pn, while the EPIC-MOS2 detector is used for the BSS. As usual a broken power law was fitted to the differential source counts:

$$\frac{dN(S)}{dS} \propto S^{-\Gamma_d} \quad S < S_b \tag{1}$$

$$\frac{dN(S)}{dS} \propto S^{-\Gamma_u} \quad S > S_b \tag{2}$$

The result of the maximum likelihood fitting yields $S_b = 1.69^{+0.02}_{-0.01} \times 10^{-14}\,\mathrm{erg\,cm^{-2}\,s^{-1}}$, with $\Gamma_d = 1.34^{+0.01}_{-0.07}$ and $\Gamma_u = 2.55^{+0.03}_{-0.04}$. The fact, already seen in other bands, that the source counts flatten from euclidean ($\Gamma_u \sim 2.5$) to highly sub-euclidean implies that most of the contribution to the XRB in this band arises from sources around S_b (see Fig. 1). Ebrero et al. (2006, this volume) discuss source counts in other X-ray bands.

3.2. The identified sources

The 242 identified sources have been classified solely in terms of their optical spectrum. Extragalactic sources have been divided in Broad-line Active Galactic Nuclei (BLAGN) when permitted lines are broader than 2000 $\mathrm{km\,s^{-1}}$, Narrow-line Emission Galaxies (NELG) when emission lines are narrower than the above limit, and Absorption Line Galaxies (ALG) when no emission line can be detected. One of the ALGs is a catalogued BL Lac and therefore is classified as such. At least two of the X-ray sources where the counterpart is an ALG show some evidence of a galaxy overdensity, and therefore could be groups or clusters. We do not separate clusters as a subclass any further, as this will require a proper assessment on whether the X-ray source is extended or not and a proper quantification of galaxy number densities around all sources. This work is now in progress. Finally, a number of stars were found as counterparts. Table 2 shows the breakdown of the identified sources.

Table 2. Breakdown of XMS identifications. Percentages refer to the identified sources (242)

Source Class	Number	%
Total id	242	100
BLAGN	178	74
NELG	37	15
ALG	8	4
Stars	18	7
BL Lac	1	0

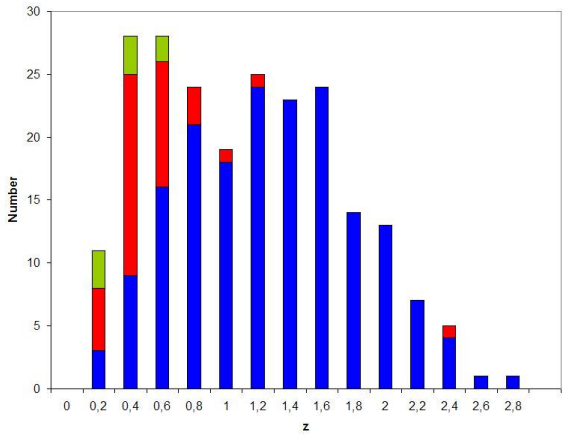

Figure 3. Redshift distribution of the extragalactic component of the sources identified in the XMS. Dark is for BLAGN, lighter for NELG and still lighten for ALG.

The results from the identifications conducted so far reveal that BLAGN dominate the source population at this flux limit. The X-ray luminosity of all of the extragalactic sources, but one ALG, is in excess of $10^{42}\,\mathrm{erg\,s^{-1}}$ and are therefore consistent with being powered by an AGN. Assuming that NELG and ALG are obscured AGN, they represent 25% of the whole AGN population at this flux level.

The redshift distribution of the XMS sources identified as extragalactic is shown in Fig. 3. We see that most of the "obscured" AGN lie at relatively low redshift, although a few high-luminosity examples of these (i.e., type 2 QSOs) are also found in the sample.

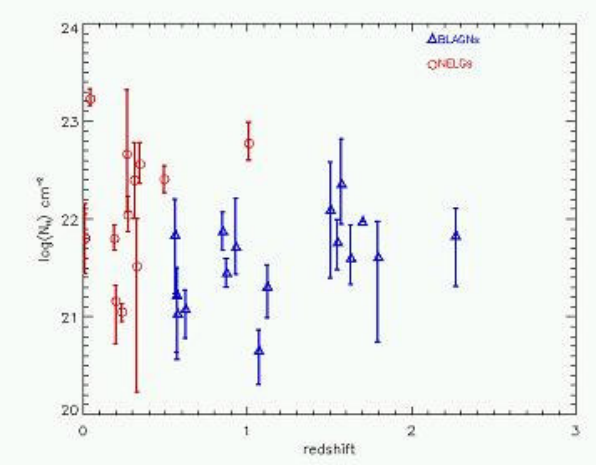

Figure 4. Intrinsic absorption column density versus redshift for those AGN where absorption is detected. Adapted from Mateos et al. (2005).

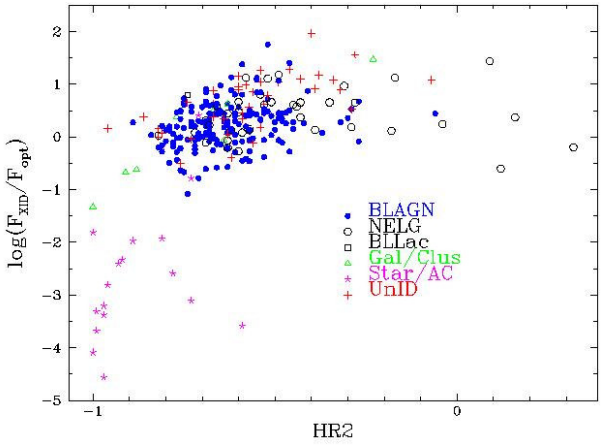

Figure 5. X-ray to optical flux ratio as a function of the hardness ratio HR_2. Symbols as in figure 1.

3.3. X-ray spectral properties of XMS sources

Mateos et al (2004) have studied the X-ray spectral properties of a superset of the XMS sample, consisting of ~ 1000 X-ray sources with fairly good spectral quality. The main results from that work are that a fraction $< 10\%$ of the BLAGN are moderately absorbed in X-rays, and that in the NELGs absorption is common, typically with higher column densities, but not universal. Fig. 4 illustrates this. These results are consistent with previous work from Piconcelli et al (2002) and have been confirmed by Mateos et al (2006) from the study of the much better quality X-ray spectra of serendipitous sources in the Lockman Hole.

A lot of excitement has recently arisen on the detection of a large equivalent width Fe emission line in the average, de-redshifted spectra of type 1 and type 2 AGN. The results from Streblyanska et al (2005), based on XMM-Newton observations of the Lockman Hole, are now at least qualitatively confirmed by Brusa et al (2005) using Chandra data. Corral et al. (2006, this volume) report on preliminary results from a similar exercise conducted with the XMS. Although the quality of individual spectra is much lower than that of the Lockman Hole survey, the number of BLAGN is much larger. These preliminary results appear to indicate an Fe line in the average spectra too, again in qualitative agreement with previous work.

4. TIPS FOR STATISTICAL IDENTIFICATION

Although the incompleteness in the identifications of the XMS, with a bias against high X-ray to optical flux ratio sources, prevents us from computing X-ray luminosity functions and other overall statistical descriptors of the sample itself, other applications can be already explored at its current stage. In what follows we will present a few preliminary tips on the classification of XMS sources, based on X-ray properties and optical photometric properties. The ultimate goal of all this is to develop a statistical identification tool, whereby X-ray sources in the XMM-Newton source catalogue can be classified without the costly optical spectroscopy in hand. In a second step, and with enough optical photometric data available, even approximate redshifts could be obtained.

To properly develop a statistical identification tool will ultimately require some sort of mathematical algorithm like a principal component analysis, an artificial neural network or some other sophisticated tool. This is well beyond the scope of the present discussion, where we only aim at exploring the parameter space in the search of potentially interesting quantities that can guide the statistical identification process.

The first diagram we explore is the X-ray to optical flux ratio versus X-ray hardness ratio HR_2 defined as

$$HR_2 = \frac{H - S}{H + S} \tag{3}$$

where H and S are the exposure-time corrected count rates in the 2-4.5 keV and 0.5-2 keV bands respectively. Fig. 5 shows the location of XMS sources in this diagram, already used by Della Ceca et al (2004). This diagram is very useful indeed to separate the stars from the sample, as all sources with $F_X/F_{opt} < 0.1$ are either stars or ALGs. Stars are the only point-like objects in this part of the diagram, the remainder being ALGs. Only 2 out of our 18 stars do not reside in this part of the diagram.

The very soft ($HR_2 < -0.85$) part of this diagram at larger F_X/F_{opt} is dominantly populated by ALGs. In these sources it is likely that a soft excess possibly due to the host galaxy provides an important contribution to the X-ray spectrum, although most likely the majority of the X-ray flux is dominated by an AGN, given the large X-ray to optical flux ratio.

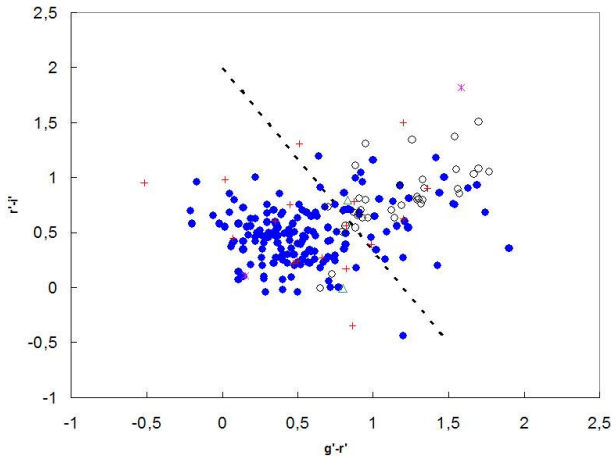

Figure 6. Optical colour-colour diagram for XMS sources. The dotted line separates approximately the QSO and emission line galaxy location (bottom left) from the early type galaxy location (top right) in the SDSS. Labels as in fig. 1.

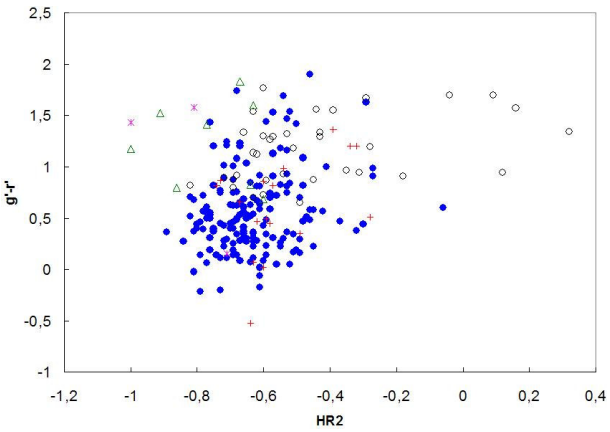

Figure 7. Optical colour versus X-ray hardness ratios of XMS sources. Labels as in fig. 1.

Working from the opposite end in HR_2, all sources with $HR_2 > 0$ are NELGs. When going to lower values of HR_2, the contamination from BLAGN starts to appear, possibly because some of them display photoelectric absorption as discussed in section 3.2. At $HR_2 > -0.4$ and $F_X/F_{opt} > 0.1$ only $> 50\%$ of the objects are NELGs and $> 20\%$ are BLAGN.

A further parameter space worth inspecting is the optical colour-colour diagram (Fig. 6). Since these are Sloan colours, we can compare the location of our sources with those from the SDSS as in Barcons et al (2002). The dotted line separates the expected location of blue galaxies (QSOs and emission line galaxies) from that of red early type galaxies in the SDSS. Barcons et al (2002) noted in their much more reduced XMS sample that the optically red part of that diagram was almost entirely populated by NELGs. With our current sample we now see that optically red objects are almost 50/50 BLAGNs and NELG+ALG. In fact, about 10% of our BLAGN are red. A preliminary inspection does not show a one to one relation between red and X-ray absorbed BLAGN, but this needs more work. The optically blue part of this diagram is, however, almost entirely populated by BLAGN, but still with some exceptions, like 10% of the NELGs.

We finally inspect an optical colour vs X-ray hardness ratio diagram, as shown in Fig. 7. Not surprisingly the blue part of this diagram is almost entirely populated by BLAGN (again with a few exceptions), but the red part shows some interesting hints. In fact, the combination of red and hard picks up almost nothing but NELGs, and the red and soft part is especially rich in ALGs.

5. OUTLOOK

We have presented preliminary results on the XMS. Although incomplete optical identification prevents us from reaching stronger conclusions, we foresee directions where progress can be made in the immediate future, concerning statistical identification. The parameter space that can be built with X-ray and optical photometric parameters only is huge, and we have explored some interesting subspaces. What we have explored so far indicates that a classification based on a few parameters like F_X/F_{opt}, HR_2, extent of the optical counterpart, $g' - r'$ and $r' - i'$ can yield without much sophistication to a classification of serendipitous X-ray sources which is reliable to $> 90\%$. In the near future we will cover this with the appropriate mathematical apparatus to provide a preliminary statistical identification tool for the XMM-Newton source catalogue. Unfortunately, photometric redshifts do not appear to work with our limited set of optical filters, even by reducing the number of templates in view of the classification of the source.

ACKNOWLEDGMENTS

We are grateful to a large number of people for a long-standing collaboration in building the XMS, including the AXIS collaboration and to the full XMM-Newton Survey Science Centre. Special thanks are due to S. Mateos, A. Corral, F. Panessa, J. Ebrero, M.J. Page, A. Schwope, M.G. Watson, R. Della Ceca, J.A. Tedds, W. Yuan, R.G. McMahon and T. Maccacaro. Partial financial support was provided by the Spanish Ministerio de Educación y Ciencia, under project ESP2003-00812.

REFERENCES

[1] Barcons, X., et al., 2002, A&A, 382, 522

[2] Brandt, W.N. & Hasinger G., 2005, ARAA, 43, 827

[3] Brusa, M., Gilli, R., Comastri, A., 2005, ApJ, 621, L5

[4] Caccianiga, A., et al., 2004, A&A, 416, 201

[5] Corral, A., et al, 2006, these proceedings

[6] Della Ceca, R., et al., 2004, A&A, 428, 383

[7] Ebrero, J. et al., 2006, these proceedings

[8] Hasinger, G., et al., 2001, A&A, 365, L45

[9] Mateos, S. et al., 2005, A&A, 433, 855

[10] Mateos, S. et al., 2006, A&A, in the press (astro-ph/0506718)

[11] Piconcelli, E., Cappi, M., Bassani, L., Fiore, F., Di Cocco, G., Stephen, J.B., 2002, A&A, 394, 835

[12] Streblyanska A., et al., 2005, A&A, 432, 395

[13] Watson, M.G. et al., 2001, A&A, 365, L51